Estimation of hourly solar irradiation on tilted surfaces

Aleksey Belsky[1], Dmitry Glukhanich[1], Tole Sutikno[2], Mohd Hatta Jopri[3]
[1]Department of Electric Power and Electromechanics, Faculty of Energy, Saint-Petersburg Mining University, Saint-Petersburg, Russia
[2]Department of Electrical Engineering, Universitas Ahmad Dahlan, Yogyakarta, Indonesia
[3]Department of Electrical Engineering Technology, Faculty of Electrical and Electronic Engineering Technology, Universiti Teknikal Melaka, Malaysia

Article Info

Article history:

Received Apr 18, 2023
Revised May 2, 2023
Accepted May 24, 2023

Keywords:

Clearness index
Diffuse ratio
Inclined surface
NASA POWER
Solar radiation

ABSTRACT

Tilted photovoltaic panel (PVP) are extensively utilized in solar power installations. To model and design them, you must understand the solar irradiation on a tilted surface over time scales of an hour, day, week, month, or other period. However, most meteorological stations only record global horizontal irradiance (GHI). In this research, a method is proposed for translating hourly worldwide horizontal irradiation from the NASA POWER database into hourly global sun irradiation on a tilted surface utilizing regression analysis methods and numerical modeling methods based on an isotropic model of solar irradiation. In addition, this work proposes a method for establishing the regression reliance of the diffuse transmittance index on the clearness index for geographic areas where this relationship has not yet been empirically proven. To assess effectiveness, the results of the proposed technique and other authors' methods are compared with monthly average NASA POWER climatological data using evaluation methods such as mean bias error (MBE), mean absolute bias error (MABE), and root-mean-square error (RMSE). The study's findings can be used to construct, optimize, or anticipate the functioning of solar power facilities at any angle of tilt and in any geographic area.

Corresponding Author:

Mohd Hatta Jopri
Department of Electrical Engineering Technology
Faculty of Electrical and Electronic Engineering Technology, Universiti Teknikal Melaka
Melaka, Malaysia
Email: hatta@utem.edu.my

1. INTRODUCTION

Interest in using solar power plant (SPP) is continuously growing all over the world, despite the stochastic nature of solar irradiation, that affects the operation of SPP [1]–[5]. The predominant technology all over the world to transform solar energy into electrical energy today is photovoltaics [6]. Solar energy is an essential part of modern energetics [7], [8]. The application of solar energy is used in many areas of human activity, including stand-alone power systems, to provide electrical energy to small businesses and households. A number of scientists' papers are devoted to the application of SPP in the mineral resources sector: i) for stand-alone objects: gas condensate wells in the Arctic [9], stand-alone coal mines [10], [11], working sites of oil and gas fields [12]; ii) improving the quality, reliability, and efficiency of the power supply [13]–[20]; and iii) principles of creation, management, and economy of energy complexes [21]–[26].

The amount of electrical energy that is produced by the photovoltaic panel (PVP) depends on the solar irradiation entering its surface, as well as the efficiency of the equipment used to convert and transmit energy [27]. Accurate information about the amount of solar irradiation is needed for designing and optimizing electrical complexes with PVP. The amount of solar irradiation entering the PVP's surface depends on many factors: geographic location, time of year and day, weather conditions, the quality, and cleanness of the PVP, and the orientation and tilt of the PVP.

High precision and expensive measuring equipment is used to determine the amount of solar irradiation in a particular location. For these purposes, a pyranometer, or pyrheliometer, is used. But because of financial constraints and/or a lack of necessary equipment, obtaining solar irradiation data might be a difficult process, especially in developing states and far-flung regions. Because of this, the role and importance of various evaluative and theoretical methods for estimation of the amount of solar irradiation on inclined surfaces is growing.

Hourly [28], [29], daily [30]–[32], monthly [33] models of solar irradiation–depending on the goals and tasks of modeling, might be used to design and optimize SPP. For many cases, it is necessary to model exactly on hourly time scales, including the time during the full calendar year. This problem is difficult because of the stochastic nature of solar irradiation [34]. The solar irradiation that passes through the atmosphere is prone to change due to two factors: atmospheric diffusion of air/water/dust molecules and atmospheric absorption by ozone/water and carbon dioxide molecules.

A part of the solar irradiation eventually reaches the earth’s surface in the form of diffuse solar irradiation [35]. For any specific geographic location for designing and building SSP, knowledge of the global horizontal irradiance (GHI) is important, as is the solar irradiance diffused component [36]–[40]. Most SPPs have tilted PVP. However, most meteorological stations only have records of GHI, which is why it is necessary to convert horizontal solar irradiation into solar irradiation for a tilted surface, taking into account its scattered and reflected components [41].

The amount of solar irradiation for a tilted surface depends on the clearness index and diffuse transmittance index. These coefficients are usually determined empirically for each geographic location. There is a high correlation between them, but it isn’t possible to obtain a unique regression curve for all locations or latitudes [42], [43]. The scientific literature about determining the regression dependence on hourly time scales has been reviewed by the authors (Table 1 [44]–[55] (see in appendix)) using the keywords «solar radiation» OR «solar irradiation» AND «diffuse ratio» OR «diffuse transmittance index» AND «clearness index» AND «hourly» in the Scopus database. The following conclusions, which are based on a critical analysis of the literature review, might be drawn:

a. The number of works devoted to the determination and refinement of regression dependencies for the diffuse transmittance index is large.
b. Most of the regression dependencies are established based on empirical studies. But there are also dependencies that have been established through analytical studies, including dependencies that were obtained using data from the NASA POWER database [56], which is freely available.
c. For Russia and Russian latitudes (4–80°N), the amount of work devoted to the determination of regression dependencies for determining diffuse transmittance index, as well as work about the determination of the total solar irradiation coming to a tilted PVP, is too small. At the same time, in Russia, there are only about two dozen meteorological stations capable of making heliometrical observations.

2. RESEARCH METHOD

The NASA POWER project application has become widespread among scientists who are involved in research on renewable energy sources [57]. NASA POWER (prediction of worldwide energy resources) is a tool that provides global information on solar irradiation, wind, and geothermal resources obtained from satellites and available for downloading and analyzing. The tool is used for researching, planning, and developing energy projects and for evaluating the possibility of using renewable energy sources. The NASA POWER database includes long-term estimates of meteorological and solar energy flows that are provided by satellite systems. These data meet the needs of scientists and have been shown to be accurate enough to provide consistent solar and meteorological data for locations where there is little or no meteorological [58]–[60].

NASA POWER provides hourly scale information on GHI, air temperature at 2 meters, and wind speed at 10 meters. Also, information is provided on the monthly average global irradiance on a tilted surface (surface tilt angles: 0°, *latitude*−15°, *latitude*, *latitude*+15°, 90°). Since no information about solar irradiation on a tilted surface on an hourly scale is available, a method is proposed for converting hourly GHI via the NASA POWER database into hourly global irradiance on a tilted surface. The following parameters (Table 2), extracted from NASA POWER, are used as initial data for a model for estimating global irradiance on a tilted surface. The proposed method consists of three steps.

Table 2. Initial data description from the NASA POWER database

No	Parameter	Description
1	All sky surface shortwave downward irradiance Scales: hourly, monthly	The total solar irradiation (direct plus diffuse) incident in a horizontal plane on the earth's surface under all sky conditions (GHI).
2	All sky insolation clearness index (k_t) Scales: hourly	A coefficient that represents the clarity of the atmosphere is the ratio of the global sky insolation that is transmitted through the atmosphere to reach the earth's surface to the average value of the global solar irradiation falling on the top of the atmosphere.
3	All sky surface albedo Scales: hourly	The reflection coefficient of the earth's surface over the entire sky is the ratio of solar irradiation reflected by the earth's surface to the total amount of incident solar irradiation reaching the earth's surface.
4	Integrated solar zenith angle Scales: hourly	The angle between sunbeams and vertical direction.
5	Top-of-atmosphere shortwave downward irradiance (*toa*) Scales: monthly	The total solar irradiation on the horizontal plane at the top of the atmosphere (extraterrestrial irradiation).
6	All sky surface shortwave diffuse irradiance Scales: monthly	The diffuse irradiation on the earth's surface in a horizontal plane under any sky conditions.

2.1. Determination of the sun's position

Foremost, it is necessary to make calculations to determine the sun's position on an hourly scale. Widely known methods are used to perform these calculations [61]. At twelve o'clock local solar time (LST), the sun is at its highest position in the sky. This time is usually different from local time (LT), due to the earth's curved orbit, time zones, and daylight savings time. The meridian of local standard time meridian (LSTM) is used as a reference point for a certain time zone, which is determined as (1):

$$LSTM = 15° \cdot \Delta T_{UTC} \tag{1}$$

where ΔT_{UTC} is the difference in hours between LT and universal time (UTC).

The equation of time (EoT) takes into account the fact that the earth's orbit and its axial tilt are not perfectly round or oriented in the same direction, respectively, and is given as (2):

$$EoT = 9.87 \sin 2B - 7.53 \cos B - 1.5 \sin B \tag{2}$$

where $\mathrm{B} = 360/365(\mathrm{d} - 81)$, d is the number of the day in a year.

The time correction factor (TC) (in minutes) is used to reflect the change in LST that occurs within a particular time zone as longitude changes, and also includes the above EoT. TC is determined by as (3):

$$TC = 4(Longitude - LSTM) + EoT \tag{3}$$

where *Longitude* is the local longitude in degrees.
According to the two previous corrections, LT can be corrected to obtain LST by as (4):

$$LST = LT + \frac{TC}{60} \tag{4}$$

The hour angle (HRA) is used to convert the passage of time into a measure of the sun's position in the sky in degrees. At noon, when the sun is in its highest position in the sky, it will always be 0°. The sun moves across the sky at an angular velocity of 15° per hour. Before noon, this equates to a negative HRA, and after noon, the HRA will be positive. HRA is determined as (5):

$$\mathrm{HRA} = 15°(\mathrm{LST} - 12) \tag{5}$$

The inclination of the earth relative to its axis results in a change in the angle of declination, denoted by δ, over time. Without this slope, the declination angle would remain at 0°. However, since the earth is tilted by 23.45°, the declination can vary plus or minus that amount. On the spring and autumn equinox days, the declination returns to 0°. To calculate the angle of declination of the sun, the expression (6) should be used.

$$\delta = 23.45 \sin\left(\frac{360}{365}\right) \cdot (d + 284) \tag{6}$$

The angle of the sun's elevation is the angular measurement of the sun's position in the sky relative to the horizon. The zenith angle is the angle of elevation of the sun relative to the vertical. This angle is taken from the NASA POWER database for modeling. Thus, the angle of the sun's elevation is the zenith angle, as indicated as (7):

$$\alpha = 90° - \zeta \tag{7}$$

where ζ is the solar zenith angle.

The azimuthal angle from which the sun's rays reach the earth changes during the day and depends on the latitude and time of the year. It is determined by (8). At noon in the Northern Hemisphere, the sun is in the south, and in the Southern Hemisphere, it is in the north.

$$\theta = \begin{cases} arccos\left(\frac{sin\,\delta \cdot cos\,Latitude - cos\,\delta \cdot sin\,Latitude \cdot cos\,HRA}{cos\,\alpha}\right) & LST < 12,\ HRA < 0 \\ 360° - arccos\left(\frac{sin\,\delta \cdot cos\,Latitude - cos\,\delta \cdot sin\,Latitude \cdot cos\,HRA}{cos\,\alpha}\right) & LST \geq 12,\ HRA \geq 0 \end{cases} \tag{8}$$

The angle of sunlight incidence on the PVP is determined as (9):

$$AOI = arccos(cos\quad \zeta \cdot cos\,\beta + sin\,\zeta \cdot sin\,\beta \cdot cos(\theta - \phi)) \tag{9}$$

where β is the PVP tilt angle; ϕ is the azimuth angle of the PVP direction.

2.2. Estimate of diffuse transmittance index

The diffuse transmittance index (K_d) is defined as a function of the clearness index (K_t). Typically, the diffuse transmittance index is determined empirically for every geographic location. In this study, it is proposed to define the diffuse transmittance index as a function of the clearness index based on NASA POWER statistics data for the observation period 2001-2021.

The following parameters are retrieved from the NASA POWER database on a monthly measurement scale: i) GHI; ii) top of atmosphere irradiance (TOA); and iii) diffuse horizontal irradiance (DHI). The values of the clearness index and diffuse transmittance index are found for the monthly average values of GHI, TOA, and DHI for each year from 2001 to 2021, according to as (10) and (11):

$$K_t = \frac{GHI}{TOA} \tag{10}$$

$$K_d = \frac{DHI}{GHI} \tag{11}$$

According to the expressions, 252 points are obtained that characterize the dependence of the diffuse transmittance on the sky purity index. A regression dependence $K_d = f(K_t)$ builds based on the points obtained.

2.3. Global irradiance on a tilted surface

The applied model for global irradiance on a tilted surface calculation is based on the isotropic Liu and Jordan's model [62]. Liu and Jordan's model is one of the first and simplest models of solar irradiation, and this model is recognized as one of the most accurate among the isotropic models of solar irradiation on a tilted surface [63]. This model assumes that the intensity of diffuse solar irradiation is evenly distributed over the entire sky and is calculated by as (12):

$$E = E_b + E_g + E_d \tag{12}$$

where E_b is normal solar irradiation, corrected for the angle of incidence, and is given by (13); E_g is reflected solar irradiation from the earth and is determined by the expression (14); and E_d is diffuse solar irradiation and is determined by as (15).

$$E_b = DNI \cdot cos(AOI) \tag{13}$$

where $DNI = \frac{GHI - DHI}{cos\,\zeta}$ is the direct normal irradiance.

$$E_g = 0.5 \cdot GHI \cdot \rho \cdot (1 - cos\,\beta) \quad (14)$$

Where GHI is the global horizontal irradiance; ρ is the albedo of a terrestrial surface.

$$E_d = 0.5DHI \cdot (1 + cos\,\beta) \quad (15)$$

Where $DHI = K_d \cdot GHI$ is the DHI and K_d is diffuse transmittance index (Liu and Jordan model [64]).

3. RESULTS AND DISCUSSION

The modeling results are presented as tables and figures for two geographic locations: Novozapolyarny (Russia) (66.74°N, 79.52°E) and Nefteyugansk (Russia) (61.088°N, 72.6133°E).

a. Example 1: estimation for Novozapolyarny: the regression dependence definition $K_d = f(K_t)$ is presented in Figure 1. In Tables 3, 4, and Figure 2, the monthly average values of global irradiance on a tilted surface for 2001–2021 are presented by the NASA POWER database and estimated values, respectively. Modeling results of global irradiance on a latitude-oriented surface during the year are presented in Figure 3.

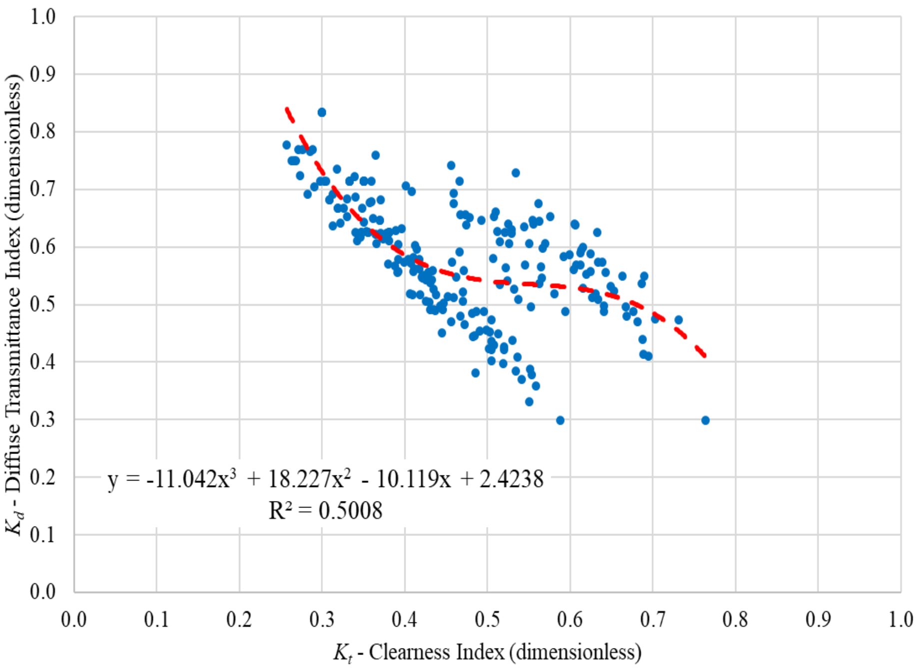

Figure 1. Determination of the diffuse transmittance index as a function of the clearness index calculated by meteorological and solar monthly and annual climatology data for 2001–2021

Table 3. Monthly average global irradiance on a tilted surface for 2001-2021 by NASA POWER, kWh/m^2/day

Month	Surface tilt angle				
	0°	*Latitude*−15°	*Latitude*	*Latitude*+15°	90°
January	0.07	0.66	0.75	0.8	0.8
February	0.69	1.81	1.96	2	1.98
March	2.34	4.09	4.25	4.21	4.1
April	4.49	5.93	5.87	5.61	5.36
May	5.24	5.54	5.21	4.74	4.41
June	5.41	5.16	4.59	3.87	3.39
July	5.13	5.04	4.52	3.84	3.38
August	3.38	3.72	3.44	3.02	2.72
September	1.92	2.61	2.53	2.33	2.17
October	0.68	1.24	1.27	1.25	1.2
November	0.16	0.75	0.83	0.87	0.86
December	0.01	0.33	0.39	0.41	0.42

Table 4. Estimated monthly average global irradiance on a tilted surface for 2001-2021, kWh/m^2/day

Month	Surface tilt angle				
	0°	*Latitude*−15°	*Latitude*	*Latitude*+15°	90°
January	0.07	0.56	0.63	0.67	0.67
February	0.69	2.10	2.29	2.35	2.33
March	2.36	4.39	4.54	4.51	4.41
April	4.48	5.90	5.83	5.64	5.47
May	5.20	5.51	5.25	4.86	4.59
June	5.52	5.12	4.56	3.84	3.39
July	5.13	4.90	4.40	3.73	3.31
August	3.39	3.62	3.34	2.91	2.63
September	1.94	2.58	2.49	2.28	2.12
October	0.69	1.29	1.33	1.30	1.26
November	0.16	0.73	0.81	0.85	0.85
December	0.01	0.35	0.41	0.43	0.44

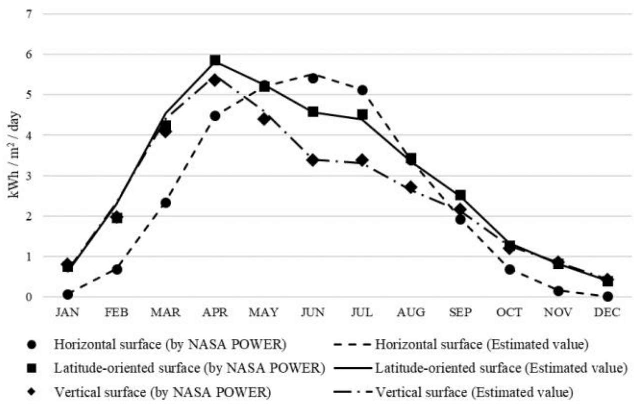

Figure 2. Monthly average global irradiance on a tilted surface for Novozapolyarny

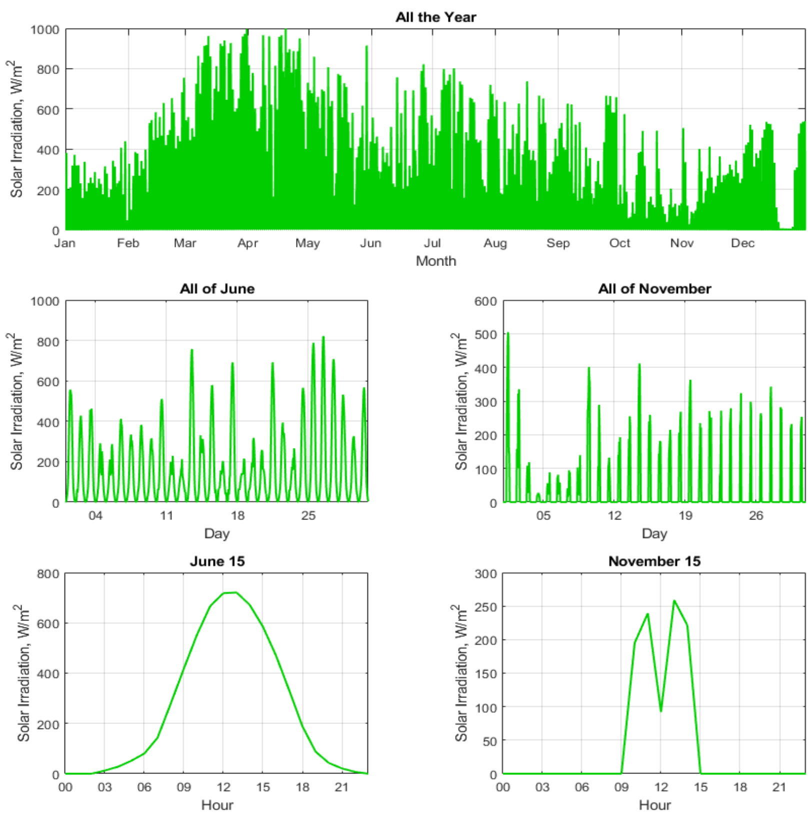

Figure 3. Hourly global irradiance on a latitude-oriented surface for Novozapolyarny

b. Example 2: estimation for Nefteyugansk: the regression dependence definition $K_d = f(K_t)$ is presented in Figure 4. In Tables 5, 6, and Figure 5, the monthly average values of global irradiance on a tilted surface for 2001–2021 are presented by the NASA POWER database and estimated values, respectively. Modeling results of global irradiance on a latitude-oriented surface during the year are presented in Figure 6.

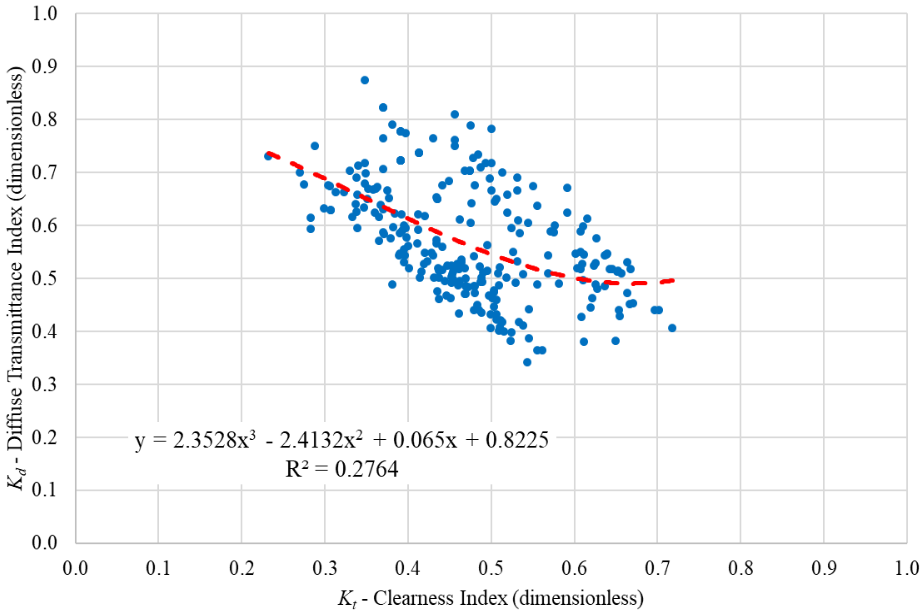

Figure 4. Determination of the diffuse transmittance index as a function of the clearness index calculated by meteorological and solar monthly and annual climatology data for 2001–2021

Table 5. Monthly average global irradiance on a tilted surface for 2001-2021 by NASA POWER, kWh/m^2/day

Month	Surface tilt angle				
	0°	*Latitude*−15°	*Latitude*	*Latitude*+15°	90°
January	0.38	1.08	1.21	1.27	1.27
February	1.2	2.55	2.76	2.83	2.77
March	2.88	4.38	4.53	4.48	4.25
April	4.44	5.43	5.3	4.98	4.51
May	5.08	5.15	4.71	4.11	3.4
June	5.45	5.14	4.56	3.83	3.01
July	5.23	5.08	4.55	3.85	3.05
August	3.75	4.03	3.73	3.27	2.71
September	2.21	2.8	2.71	2.49	2.18
October	1.01	1.59	1.63	1.58	1.47
November	0.39	0.98	1.08	1.12	1.10
December	0.19	0.63	0.71	0.75	0.75

Table 6. Estimated monthly average global irradiance on a tilted surface for 2001-2021, kWh/m^2/day

Month	Surface tilt angle				
	0°	*Latitude*−15°	*Latitude*	*Latitude*+15°	90°
January	0.38	1.50	1.72	1.83	1.84
February	1.25	2.88	3.15	3.25	3.19
March	2.90	4.52	4.68	4.64	4.42
April	4.47	5.35	5.23	4.93	4.49
May	5.01	4.98	4.55	3.97	3.31
June	5.39	5.00	4.44	3.74	2.97
July	5.17	4.92	4.40	3.73	2.99
August	3.73	3.91	3.61	3.16	2.63
September	2.26	2.85	2.76	2.54	2.23
October	1.02	1.70	1.76	1.72	1.61
November	0.39	1.12	1.25	1.31	1.29
December	0.19	1.03	1.19	1.29	1.30

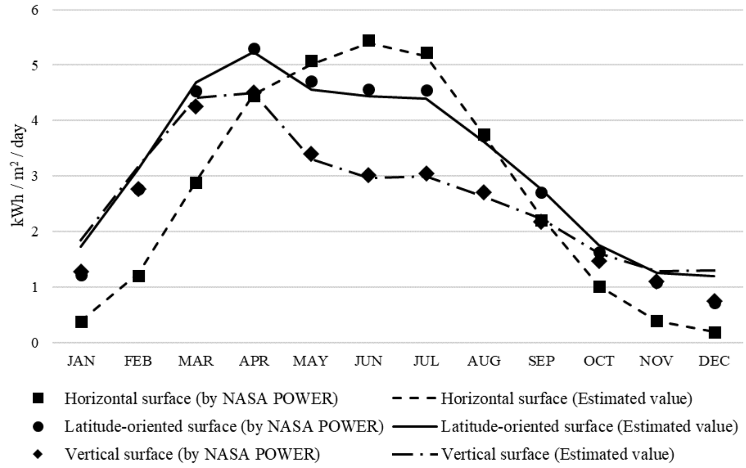

Figure 5. Monthly average global irradiance on a tilted surface for Nefteyugansk

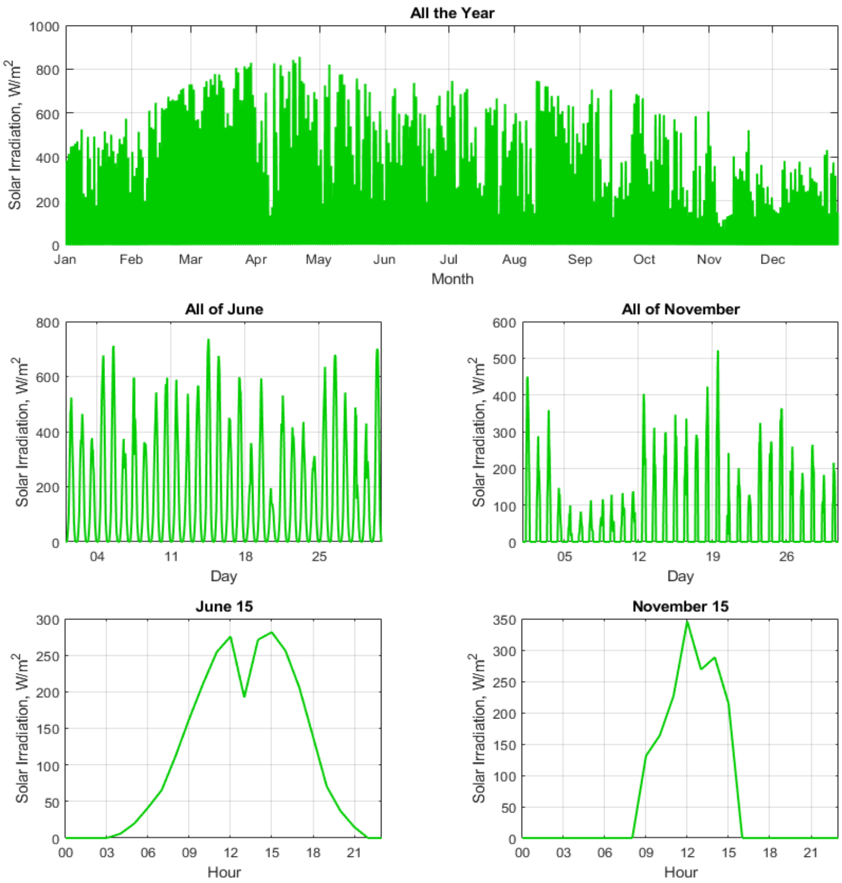

Figure 6. Hourly global irradiance on a latitude-oriented surface for Nefteyugansk

To verify the proposed method, the estimated monthly average values of global irradiance on a tilted surface are compared with the monthly average values of global irradiance for 2001-2021 according to the climatological data of the NASA POWER (surface tilt angles: 0°, *Latitude*−15°, *Latitude*, *Latitude*+15°, 90°). To estimate the effectiveness of the proposed method, the results are compared with the methods of other authors (from Table 1), which were designed for the latitude of 60°N and north. Comparisons were held on mean bias error (MBE), mean absolute bias error (MABE), and root mean squared error (RMSE) criteria. These test methods can be expressed through as (16)-(18):

$$MBE = \frac{1}{N}\sum_{i=1}^{N}(y_i - x_i),\; nMBE = \frac{MBE}{\bar{x}} \cdot 100\% \quad (16)$$

$$MABE = \frac{1}{N}\sum_{i=1}^{N}|y_i - x_i|,\; nMABE = \frac{MABE}{\bar{x}} \cdot 100\% \quad (17)$$

$$RMSE = \sqrt{\frac{1}{N}\sum_{i=1}^{N}(y_i - x_i)^2},\; nRMSE = \frac{RMSE}{\bar{x}} \cdot 100\% \quad (18)$$

where N is a number of values; x_i is the monthly average global irradiance on a tilted surface for 2001-2021 by NASA POWER database; $\bar{x}$ is the average of x_i; and y_i is the estimated monthly average values of global irradiance on a tilted surface for 2001-2021.

The better the model for estimating hourly solar radiation, the lower the values of MBE, MBE, and RMSE [65]. For global irradiance, nMBE and nMABE within ±10% and nRMSE<20% indicate good model results [66]. Comparison results are presented in Tables 7 and 8: i) model 1 is the model of the proposed authors' method; ii) model 2 is the Reindl *et al.* [46] model; iii) model 3 is the Berrizbeitia *et al.* [43] model; iv) model 4 is the Bortolini *et al.* [41] model for an annual scenario; v) model 5 is the Bortolini *et al.* [41] model for a seasonal scenario; and vi) model 6 is the Muneer *et al.* [55] model.

Table 7. Comparison of estimated models for Novozapolyarny

Parameter	Model 1	Model 2	Model 3	Model 4	Model 5	Model 6
MBE, kWh/m^2/day	0.03	0.11	-0.06	0.18	0.16	-0.06
nMBE, %	1.00	3.96	-2.15	6.53	5.80	-2.15
MABE, kWh/m^2/day	0.09	0.27	0.11	0.23	0.22	0.11
nMABE, %	3.19	9.61	4.13	8.43	8.06	4.13
RMSE, kWh/m^2/day	0.21	0.85	0.46	1.40	1.24	0.46
nRMSE, %	7.73	30.65	16.67	50.56	44.89	16.63

Table 8. Comparison of estimated models for Nefteyugansk

Parameter	Model 1	Model 2	Model 3	Model 4	Model 5	Model 6
MBE, kWh/m^2/day	0.09	0.14	0.03	0.25	0.23	0.03
nMBE, %	3.15	4.73	0.92	8.58	8.06	0.92
MABE, kWh/m^2/day	0.17	0.22	0.15	0.26	0.25	0.15
nMABE, %	5.80	7.61	5.21	8.98	8.62	5.21
RMSE, kWh/m^2/day	0.71	1.06	0.21	1.92	1.81	0.21
nRMSE, %	24.39	36.61	7.09	66.48	62.46	7.13

From the comparison of estimated models for Novozapolyarny, one can see that model 1 is better than other models. From the comparison of estimated models for Nefteyugansk, one can see that model 1 is worse than model 3 and model 6, but better than model 2, model 4, and model 5. Notably, in model 3 and model 6, the diffuse transmittance index was obtained as a result of an assessment of empirically obtained data for latitudes close to the latitude of Nefteyugansk. However, Novozapolyarny is located north of Nefteyugansk, and in this case, model 1 manifests itself better than model 3 and model 6.

4. CONCLUSION

A method for converting hourly GHI to global irradiance on a slanted surface has been developed. This method makes use of publicly available data from NASA's POWER database, the well-known solar position model, and numerical modeling methods based on an isotropic model of solar irradiation. A comparison of the anticipated monthly average sun irradiation values with the monthly average solar irradiation values according to NASA POWER climatological data demonstrates good modeling results according to the MBE, MABE, and RMSE criteria.

Furthermore, a method for determining the reliance of the diffuse transmittance index on the clearness index was proposed for geographic locations where dependence had not previously been empirically demonstrated. This strategy was compared to the models of other authors using the MBE, MABE, and RMSE criteria. In modeling, the proposed strategy produces good results. The approach works best at latitudes with no experimentally confirmed dependence. However, if there is an empirically verified one, it should be used.

APPENDIX

Table 1. Hourly diffuse irradiation models

No	Authors	Regression dependency	Location	Latitude
1	Orgill and Hollands [44]	$\begin{cases} K_d = 1 - 0.249K_t & for \quad K_t < 0.35 \\ K_d = 1.157 - 1.84K_t & for \quad 0.35 \le K_t \le 0.75 \\ K_d = 0.177 & for \quad K_t > 0.75 \end{cases}$	Toronto (Canada)	43.66° N
2	Erbs *et al.* [45]	$\begin{cases} K_d = 1 - 0.099K_t & for \quad K_t < 0.22 \\ K_d = 0.9511 - 1.16K_t + 4.388{K_t}^2 - \\ -16.638{K_t}^3 + 12.336{K_t}^4 & for \quad 0.22 \le K_t \le 0.8 \\ K_d = 0.165 & for \quad K_t > 0.8 \end{cases}$	US	31°-42° N
3	Reindl *et al.* [46]	$\begin{cases} K_d = 1.02 - 0.249K_t & for \quad K_t < 0.3 \\ K_d = 1.45 - 1.67K_t & for \quad 0.3 \le K_t < 0.78 \\ K_d = 0.147K_t & for \quad K_t \ge 0.75 \end{cases}$	Europe and North America	28°-60° N
4	Hawlader [47]	$\begin{cases} K_d = 0.915K_t & for \quad K_t \le 0.225 \\ K_d = 1.135 - 0.9422K_t - 0.3878{K_t}^2 & for \quad 0.225 < K_t < 0.775 \\ K_d = 0.215K_t & for \quad K_t \ge 0.775 \end{cases}$	Singapore	1.29° N
5	Spencer [48]	$K_d = a_3 - b_3K_t - 0.3878{K_t}^2 \quad for \quad 0.35 < K_t < 0.75$	Australia	20°-42° S
6	Chandrasekaran and Kumar [49]	$\begin{cases} K_d = 1.0086 - 0.178K_t & for \quad K_t \le 0.24 \\ K_d = 0.9686 - 1.1325K_t - 1.4183{K_t}^2 + \\ +10.1862{K_t}^3 + 8.3733{K_t}^4 & for \quad 0.24 < K_t < 0.8 \\ K_d = 0.197 & for \quad K_t \ge 0.8 \end{cases}$	Madras (India)	13° N
7	Boland *et al.* [50]	$K_d = 1/[1 + \exp(-5.0033 + 8.6025K_t)]$	Australia (Victoria)	38.09° S
8	Miguel *et al.* [51]	$\begin{cases} K_d = 0.995 - 0.081K_t & for \quad K_t \le 0.21 \\ K_d = 0.724 - 2.738K_t - 8.32{K_t}^2 + \\ +4.967{K_t}^3 & for \quad 0.21 < K_t < 0.76 \\ K_d = 0.18 & for \quad K_t \ge 0.76 \end{cases}$	Greece, Portugal, France, Spain	37°-44° N
9	Oliveira *et al.* [52]	$\begin{cases} K_d = 1 & for \quad K_t \le 0.17 \\ K_d = 0.97 - 0.8K_t - 3{K_t}^2 + \\ +3.1{K_t}^3 + 5.2{K_t}^4 & for \quad 0.17 < K_t < 0.75 \\ K_d = 0.17 & for \quad K_t \ge 0.75 \end{cases}$	Sao Paulo	23.54° S
10	Karatasou *et al.* [53]	$\begin{cases} K_d = 0.9995 - 0.05K_t - 2.4156{K_t}^2 + \\ +1.4926{K_t}^3 & for \quad 0 \le K_t \le 0.78 \\ K_d = 0.2 & for \quad K_t > 0.78 \end{cases}$	Athens, Greece	37.97° N
11	Soares *et al.* [54]	$\begin{cases} K_d = 1 & for \quad K_t \le 0.17 \\ K_d = 0.90 - 1.1K_t - 4.5{K_t}^2 + \\ +0.01{K_t}^3 + 3.14{K_t}^4 & for \quad 0.17 < K_t < 0.75 \\ K_d = 0.17 & for \quad K_t \ge 0.75 \end{cases}$	Athens, Greece	37,97° N
12	Berrizbeitia *et al.* [43]	$K_d = 0.8636 - 0.9291K_t - 0.4623{K_t}^2 \quad for \quad 13 \ldots 20° N$ $K_d = 1.0815 - 1.8386K_t - 0.994{K_t}^2 \quad for \quad 20 \ldots 42° N$ $K_d = 0.9502 - 1.185K_t - 0.8896{K_t}^2 \quad for \quad 50 \ldots 58° N$	India, Kingdom of Bahrain, State of Kuwait, Spain, Portugal, United Kingdom	13°-58° N
13	Bortolini *et al.* [41]	$K_d = 0.9888 + 0.3950K_t - -3.7003{K_t}^2 + 2.2905{K_t}^3 \quad for$ annual scenario $K_d = 1.0172 + 0.0158K_t - -2.7036{K_t}^2 + 1.5729{K_t}^3 \quad for$ seasonal scenario (summer) $K_d = 0.9403 + 0.9887K_t - -5.2499{K_t}^2 + 3.4586{K_t}^3 \quad for$ seasonal scenario (winter)	Europe	37°-59° N
14	Muneer *et al.* [55]	$K_d = 0.95 - 1.185K_t - 0.89{K_t}^2$	United Kingdom	51.42° N

REFERENCES

[1] Z. S. Li, G. Q. Zhang, D. M. Li, J. Zhou, L. J. Li, and L. X. Li, "Application and development of solar energy in building industry and its prospects in China," *Energy Policy*, vol. 35, no. 8, pp. 4121–4127, 2007, doi: 10.1016/j.enpol.2007.02.006.

[2] J. Ottonelli, L. L. B. Lazaro, J. C. S. Andrade, and S. Abram, "Do solar photovoltaic clean development mechanism projects contribute to sustainable development in Latin America? Prospects for the Paris Agreement," *Energy Policy*, vol. 174, p. 113428, Oct. 2023, doi: 10.1016/j.enpol.2023.113428.

[3] O. V. Shepovalova, "Energy Saving, Implementation of Solar Energy and Other Renewable Energy Sources for Energy Supply in Rural Areas of Russia," *Energy Procedia*, vol. 74, pp. 1551–1560, 2015, doi: 10.1016/j.egypro.2015.07.718.

[4] O. I. Dranko, M. M. Dvoryashina, and Y. V. Blagodarnyy, "The Growth Assessment of Renewable Energy in Russia: The Retrospective Analysis," *IFAC-PapersOnLine*, vol. 55, no. 9, pp. 64–69, 2022, doi: 10.1016/j.ifacol.2022.07.012.

[5] S. Manju and N. Sagar, "Progressing towards the development of sustainable energy: A critical review on the current status, applications, developmental barriers and prospects of solar photovoltaic systems in India," *Renewable and Sustainable Energy Reviews*, vol. 70 , pp. 298–313, 2017, doi: 10.1016/j.rser.2016.11.226.

[6] U. Desideri and P. E. Campana, "Analysis and comparison between a concentrating solar and a photovoltaic power plant," *Applied Energy*, vol. 113, pp. 422–433, 2014, doi: 10.1016/j.apenergy.2013.07.046.

[7] V. S. Litvinenko, P. S. Tsvetkov, M. V. Dvoynikov, and G. V. Buslaev, "Barriers to implementation of hydrogen initiatives in the context of global energy sustainable development," *Journal of Mining Institute*, vol. 244, no. 4, pp. 428–438, 2020, doi:

10.31897/PMI.2020.4.5.
[8] Y. L. Zhukovskiy, D. E. Batueva, A. D. Buldysko, B. Gil, and V. V. Starshaia, "Fossil energy in the framework of sustainable development: Analysis of prospects and development of forecast scenarios," *Energies*, vol. 14, no. 17, pp. 1–28, 2021, doi: 10.3390/en14175268.
[9] G. Stroykov, A. Y. Cherepovitsyn, and E. A. Iamshchikova, "Powering Multiple Gas Condensate Wells in Russia's Arctic: Power Supply Systems Based on Renewable Energy Sources," *Resources*, vol. 9, no. 11, p. 130, Nov. 2020, doi: 10.3390/resources9110130.
[10] J. D. Ampah *et al.*, "Performance analysis and socio-enviro-economic feasibility study of a new hybrid energy system-based decarbonization approach for coal mine sites," *Science of The Total Environment*, vol. 854, p. 158820, Jan. 2023, doi: 10.1016/j.scitotenv.2022.158820.
[11] M. A. Vasilyeva, A. A. Volchikhina, and M. D. Morozov, "Re-backfill technology and equipment," *MIAB. Mining informational and analytical bulletin*, no. 6, pp. 133–144, 2021, doi: 10.25018/0236_1493_2021_6_0_133.
[12] I. N. Voytyuk, A. V. Kopteva, and A. N. Skamyin, "'Emergency Response Plan' Automated System for Oil Production and Transportation Enterprises," *Journal of Ecological Engineering*, vol. 22, no. 1, pp. 76–82, 2020, doi: 10.12911/22998993/128871.
[13] K. V. Babyr, D. A. Ustinov, and D. N. Pelenev, "Improving Electrical Safety of the Maintenance Personnel in the Conditions of Incomplete Single-Phase Ground Faults," *Occupational Safety in Industry*, no. 8, pp. 55–61, Aug. 2022, doi: 10.24000/0409-2961-2022-8-55-61.
[14] Y. A. Sychev and R. Y. Zimin, "Improving the quality of electricity in the power supply systems of the mineral resource complex with hybrid filter-compensating devices," *Journal of Mining Institute*, vol. 247, no. 1, pp. 132–140, 2021, doi: 10.31897/PMI.2021.1.14.
[15] Y. A. Sychev, V. N. Kostin, V. A. Serikov, and M. E. Aladin, "Nonsinusoidal modes in power-supply systems with nonlinear loads and capacitors in mining," *MIAB. Mining Inf. Anal. Bull.*, no. 1, pp. 159–179, 2023, doi: 10.25018/0236_1493_2023_1_0_159.
[16] Y. Shklyarskiy, I. Dobush, M. J. Carrizosa, V. Dobush, and A. Skamyin, "Method for Evaluation of the Utilitys' and Consumers'' Contribution to the Current and Voltage Distortions at the PCC," *Energies*, vol. 14, no. 24, pp. 1–21, 2021, doi: 10.3390/en14248416.
[17] M. Z. R. Z. Ahmadi, A. Jidin, M. H. Jopri, and R. N. P. Nagarajan, "Minimization of torque ripple utilizing by 3-L CHMI in DTC," *Proceedings of the 2013 IEEE 7th International Power Engineering and Optimization Conference, PEOCO 2013*, pp. 636–640, doi: 10.1109/PEOCO.2013.6564625.
[18] L. R. L. V. Raj, A. Jidin, C. W. M. F. C. W. M. Zalani, K. A. Karim, G. W. Yen, and M. H. Jopri, "Improved performance of DTC of five-phase induction machines," in *2013 IEEE 7th International Power Engineering and Optimization Conference (PEOCO)*, IEEE, 2013, pp. 613–618. doi: 10.1109/PEOCO.2013.6564621.
[19] S. Zainuddin, N. U. R. E. A. B. D. Rashid, I. P. Ibrahim, R. S. A. R. Abdullah, and Z. I. Khan, "Spectrum averaging in a MIMO FMCW maritime radar for a small fluctuating target range estimation," *Journal of Engineering Science and Technology*, vol. 17, no. 5, pp. 3342–3359, 2022.
[20] M. S. Hamid, N. Abd Manap, R. A. Hamzah, A. F. Kadmin, S. F. Abd Gani, and A. I. Herman, "A new function of stereo matching algorithm based on hybrid convolutional neural network," *Indonesian Journal of Electrical Engineering and Computer Science*, vol. 25, no. 1, pp. 223–231, 2022.
[21] R. A. Hamzah, M. S. Hamid, A. F. Kadmin, and S. F. Abd Ghani, "Improvement of stereo corresponding algorithm based on sum of absolute differences and edge preserving filter," in *2017 IEEE International Conference on Signal and Image Processing Applications (ICSIPA)*, IEEE, 2017, pp. 222–225.
[22] T. N. S. T. Zawawi, A. R. Abdullah, M. H. Jopri, T. Sutikno, N. M. Saad, and R. Sudirman, "A review of electromyography signal analysis techniques for musculoskeletal disorders," *Indonesian Journal of Electrical Engineering and Computer Science*, vol. 11, no. 3, pp. 1136–1146, 2018, doi: 10.11591/ijeecs.v11.i3.pp1136-1146.
[23] Y. E. Shklyarskiy and D. E. Batueva, "Operation mode selection algorithm development of a wind-diesel power plant supply complex," *Journal of Mining Institute*, vol. 253, no. 1, pp. 115–126, 2022, doi: 10.31897/PMI.2022.7.
[24] V. A. Shpenst and E. A. Orel, "Improving the reliability of DC-DC power supply by reserving feedback signals," *Energetika. Proceedings of CIS Higher Education Institutions and Power Engineering Associations*, vol. 64, no. 5, pp. 408–420, 2021, doi: 10.21122/1029-7448-2021-64-5-408-420.
[25] Y. E. Shklyarskiy, D. D. Guerra, E. V Iakovleva, and A. Rassõlkin, "The influence of solar energy on the development of the mining industry in the Republic of Cuba," *Journal of Mining Institute*, vol. 249, pp. 427–440, 2021.
[26] S. F. Abd Gani, M. F. Miskon, and R. A. Hamzah, "Depth Map Information from Stereo Image Pairs using Deep Learning and Bilateral Filter for Machine Vision Application," in *2022 IEEE 5th International Symposium in Robotics and Manufacturing Automation (ROMA)*, IEEE, 2022, pp. 1–6.
[27] C. Mohammed *et al.*, "Extended method for the sizing, energy management, and techno-economic optimization of autonomous solar Photovoltaic/Battery systems: Experimental validation and analysis," *Energy Conversion and Management*, vol. 270, no. 6, p. 116267, 2022, doi: 10.1016/j.enconman.2022.116267.
[28] J. del Campo-Ávila, A. Takilalte, A. Bifet, and L. Mora-López, "Binding data mining and expert knowledge for one-day-ahead prediction of hourly global solar radiation," *Expert Systems with Applications*, vol. 167, p. 114147, 2021, doi: 10.1016/j.eswa.2020.114147.
[29] W. B. W. Nik, M. Z. Ibrahim, K. B. Samo, and A. M. Muzathik, "Monthly mean hourly global solar radiation estimation," *Solar Energy*, vol. 86, no. 1, pp. 379–387, 2012, doi: 10.1016/j.solener.2011.10.008.
[30] A. Manzano, M. L. Martín, F. Valero, and C. Armenta, "A single method to estimate the daily global solar radiation from monthly data," *Atmospheric Research*, vol. 166, pp. 70–82, 2015, doi: 10.1016/j.atmosres.2015.06.017.
[31] H. Zang, X. Jiang, L. L. Cheng, F. Zhang, Z. Wei, and G. Sun, "Combined empirical and machine learning modeling method for estimation of daily global solar radiation for general meteorological observation stations," *Renewable Energy*, vol. 195, pp. 795–808, 2022, doi: 10.1016/j.renene.2022.06.063.
[32] M. K. Nematchoua, J. A. Orosa, and M. Afaifia, "Prediction of daily global solar radiation and air temperature using six machine learning algorithms; a case of 27 European countries," *Ecological Informatics*, vol. 69, 2022, doi: 10.1016/j.ecoinf.2022.101643.
[33] T. R. Ayodele and A. S. O. Ogunjuyigbe, "Prediction of monthly average global solar radiation based on statistical distribution of clearness index," *Energy*, vol. 90, pp. 1733–1742, 2015, doi: 10.1016/j.energy.2015.06.137.
[34] S. Kaplanis and E. Kaplani, "Stochastic prediction of hourly global solar radiation for Patra, Greece," *Applied Energy*, vol. 87, no. 12, pp. 3748–3758, 2010, doi: 10.1016/j.apenergy.2010.06.006.
[35] K. Bakirci, "Evaluation of models for prediction of diffuse solar radiation and comparison with satellite values," *Journal of*

Cleaner Production, vol. 374, 2022, doi: 10.1016/j.jclepro.2022.133892.
[36] I. Karakoti, B. Pande, and K. Pandey, "Evaluation of different diffuse radiation models for Indian stations and predicting the best fit model," *Renewable and Sustainable Energy Reviews*, vol. 15, no. 5, pp. 2378–2384, 2011, doi: 10.1016/j.rser.2011.02.020.
[37] H. Li, X. Bu, Z. Long, L. Zhao, and W. Ma, "Calculating the diffuse solar radiation in regions without solar radiation measurements," *Energy*, vol. 44, no. 1, pp. 611–615, 2012, doi: 10.1016/j.energy.2012.05.033.
[38] T. E. Boukelia, M. S. Mecibah, and I. E. Meriche, "General models for estimation of the monthly mean daily diffuse solar radiation (Case study: Algeria)," *Energy Conversion and Management*, vol. 81, pp. 211–219, 2014, doi: 10.1016/j.enconman.2014.02.035.
[39] K. K. Gopinathan and A. Soler, "Diffuse radiation models and monthly-average, daily, diffuse data for a wide latitude range," *Energy*, vol. 20, no. 7, pp. 657–667, 1995, doi: 10.1016/0360-5442(95)00004-Z.
[40] K. Ulgen and A. Hepbasli, "Diffuse solar radiation estimation models for Turkey's big cities," *Energy Conversion and Management*, vol. 50, no. 1, pp. 149–156, 2009, doi: 10.1016/j.enconman.2008.08.013.
[41] M. Bortolini, M. Gamberi, A. Graziani, R. Manzini, and C. Mora, "Multi-location model for the estimation of the horizontal daily diffuse fraction of solar radiation in Europe," *Energy Conversion and Management*, vol. 67, pp. 208–216, 2013, doi: 10.1016/j.enconman.2012.11.008.
[42] H. Khorasanizadeh and K. Mohammadi, "Diffuse solar radiation on a horizontal surface: Reviewing and categorizing the empirical models," *Renewable and Sustainable Energy Reviews*, vol. 53, pp. 338–362, 2016, doi: 10.1016/j.rser.2015.08.037.
[43] S. E. Berrizbeitia, E. J. Gago, and T. Muneer, "Empirical Models for the Estimation of Solar Sky-Diffuse Radiation. A Review and Experimental Analysis," *Energies*, vol. 13, no. 3, pp. 1-23, Feb. 2020, doi: 10.3390/en13030701.
[44] J. F. Orgill and K. G. T. Hollands, "Correlation equation for hourly diffuse radiation on a horizontal surface," *Solar Energy*, vol. 19, no. 4, pp. 357–359, 1977, doi: 10.1016/0038-092X(77)90006-8.
[45] D. G. Erbs, S. A. Klein, and J. A. Duffie, "Estimation of the diffuse radiation fraction for hourly, daily and monthly-average global radiation," *Solar Energy*, vol. 28, no. 4, pp. 293–302, 1982, doi: 10.1016/0038-092X(82)90302-4.
[46] D. T. Reindl, W. A. Beckman, and J. A. Duffie, "Diffuse fraction correlations," *Solar Energy*, vol. 45, no. 1, pp. 1–7, 1990, doi: 10.1016/0038-092X(90)90060-P.
[47] M. N. Hawlader, "Diffuse, global and extra-terrestrial solar radiation for Singapore," *International Journal of Ambient Energy*, vol. 5, no. 1, pp. 31–38, 1984, doi: 10.1080/01430750.1984.9675406.
[48] J. W. Spencer, "A comparison of methods for estimating hourly diffuse solar radiation from global solar radiation," *Solar Energy*, vol. 29, no. 1, pp. 19–32, 1982, doi: 10.1016/0038-092X(82)90277-8.
[49] J. Chandrasekaran and S. Kumar, "Hourly diffuse fraction correlation at a tropical location," *Solar Energy*, vol. 53, no. 6, pp. 505–510, 1994, doi: 10.1016/0038-092X(94)90130-T.
[50] J. Boland, L. Scott, and M. Luther, "Modelling the diffuse fraction of global solar radiation on a horizontal surface," *Environmetrics*, vol. 12, no. 2, pp. 103–116, 2001, doi: 10.1002/1099-095X(200103)12:2<103::AID-ENV447>3.0.CO;2-2.
[51] A. De Miguel, J. Bilbao, R. Aguiar, H. Kambezidis, and E. Negro, "Diffuse solar irradiation model evaluation in the North Mediterranean Belt area," *Solar energy*, vol. 70, no. 2, pp. 143–153, 2001, doi: 10.1016/S0038-092X(00)00135-3.
[52] A. P. Oliveira, J. F. Escobedo, A. J. Machado, and J. Soares, "Correlation models of diffuse solar-radiation applied to the city of São Paulo, Brazil," *Applied Energy*, vol. 71, no. 1, pp. 59–73, 2002, doi: 10.1016/S0306-2619(01)00040-X.
[53] S. Karatasou, M. Santamouri, and V. Geros, "Analysis of experimental data on diffuse solar radiation in Athens, Greece, for building applications," *International Journal of Sustainable Energy*, vol. 23, no. 1–2, pp. 1–11, 2003, doi: 10.1080/0142591031000148597.
[54] J. Soares, A. P. Oliveira, M. Z. Božnar, J. F. Escobedo, P. Mlakar, and A. J. Machado, "Neural Network Technique Applied To Estimate Hourly Diffuse," in *Meteorologia e o Desenvolvimento Sustentável: Anais.*, 2004.
[55] T. Muneer, S. Etxebarria, and E. J. Gago, "Monthly averaged-hourly solar diffuse radiation model for the UK," *Building Services Engineering Research and Technology*, vol. 35, no. 6, pp. 573–584, 2014, doi: 10.1177/0143624414522639.
[56] NASA, "NASA POWER | Prediction Of Worldwide Energy Resources," *NASA.* https://power.larc.nasa.gov/ (access date: Feb. 01, 2023).
[57] A. B. Owolabi, B. E. K. Nsafon, and J. S. Huh, "Validating the techno-economic and environmental sustainability of solar PV technology in Nigeria using RETScreen Experts to assess its viability," *Sustainable Energy Technologies and Assessments*, vol. 36, no. September, pp. 1–11, 2019, doi: 10.1016/j.seta.2019.100542.
[58] S. Sinha and S. S. Chandel, "Prospects of solar photovoltaic-micro-wind based hybrid power systems in western Himalayan state of Himachal Pradesh in India," *Energy Conversion and Management*, vol. 105, pp. 1340–1351, 2015, doi: 10.1016/j.enconman.2015.08.078.
[59] P. Upadhyay, S. Pulipaka, M. Sharma, and R. Kumar, "A proposed maximum power point operating strategy for photovoltaic applications using monthly irradiance estimates," *Solar Energy*, vol. 141, pp. 266–277, 2017, doi: 10.1016/j.solener.2016.11.046.
[60] K. K. M. Shariff, S. Zainuddin, N. H. A. Aziz, N. E. Abd Rashid, and N. A. Z. Zakaria, "Spectral estimator effects on accuracy of speed-over-ground radar," *International Journal of Electrical and Computer Engineering (IJECE)*, vol. 12, no. 4, pp. 3900–3910, 2022.
[61] D. R. Myers, *Solar radiation: Practical modeling for renewable energy applications*. 2017. doi: 10.1201/b13898.
[62] B. Y. H. Liu and R. C. Jordan, "Daily insolation on surfaces tilted towards equator," *ASHRAE*, vol. 10, pp. 53–59, 1961.
[63] S. A. M. Maleki, H. Hizam, and C. Gomes, "Estimation of hourly, daily and monthly global solar radiation on inclined surfaces: Models re-visited," *Energies*, vol. 10, no. 1, p. 134, 2017, doi: 10.3390/en10010134.
[64] B. Y. H. Liu and R. C. Jordan, "The interrelationship and characteristic distribution of direct, diffuse and total solar radiation," *Solar Energy*, vol. 4, no. 3, pp. 1–19, 1960, doi: 10.1016/0038-092X(60)90062-1.
[65] C. A. Gueymard and D. R. Myers, "Validation and Ranking Methodologies for Solar Radiation Models," in *Modeling Solar Radiation at the Earth's Surface*, Berlin, Heidelberg: Springer Berlin Heidelberg, 2008, pp. 479–510. doi: 10.1007/978-3-540-77455-6_20.
[66] V. Badescu *et al.*, "Computing global and diffuse solar hourly irradiation on clear sky. Review and testing of 54 models," *Renewable and Sustainable Energy Reviews*, vol. 16, no. 3, pp. 1636–1656, 2012, doi: 10.1016/j.rser.2011.12.010.

BIOGRAPHIES OF AUTHORS

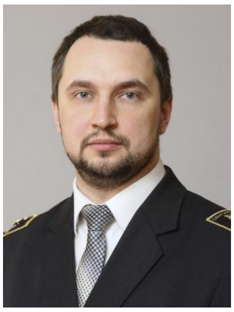

Aleksey Belsky was born in Kingisepp, Russia in 1987. He received his Bachelor of Engineering, Master of Engineering, and Ph.D. degree in Electrical Engineering from Saint-Petersburg Mining University (Russia) in 2008, 2010, and 2013, respectively. From 2013 till 2017 he was the assistant in Saint-Petersburg Mining University (Russia). Since 2017, he is an associated professor in Saint-Petersburg Mining University (Russia). His research interests include renewable energy, stand-alone power supply, solar energy, wind power, and electricity storage systems. He can be contacted at email: Belskiy_AA@pers.spmi.ru.

Dmitry Glukhanich was born in Pyt-Yakh, Russia in 1996. He received his Bachelor of Engineering, Master of Engineering in Electrical Engineering from Saint Petersburg Mining University (Russia) in 2018 and 2020, respectively. He has been a Ph.D. student in Electrical Engineering at Saint Petersburg Mining University (Russia) since 2020. His research interests are renewable energy, stand-alone power supply, solar energy, and thermoelectricity. He can be contacted at email: Glukhanich_DYu@pers.spmi.ru.

Tole Sutikno is a lecturer, and serves as the head of the Department of Electrical Engineering, as well as the head of the Master Program of Electrical Engineering within the Faculty of Industrial Technology at Universitas Ahmad Dahlan (UAD) in Yogyakarta, Indonesia. In 1999, 2004, and 2016, he graduated with a Bachelor of Engineering from Universitas Diponegoro, a Master of Engineering from Universitas Gadjah Mada, and a Doctor of Philosophy in Electrical Engineering from Universiti Teknologi Malaysia. All three degrees are in the field of electrical engineering. Since the year 2008, he has held the position of Associate Professor at the Universitas Ahmad Dahlan in Yogyakarta, Indonesia. He is among the top 2% of researchers named by Stanford University and Elsevier BV as the most influential scientists in the world for 2021–present. His research interests include the areas of digital design, industrial applications, industrial electronics, industrial informatics, power electronics, motor drives, renewable energy, FPGA applications, embedded systems, artificial intelligence, intelligent control, digital libraries, and information technology. He can be contacted at email: tole@te.uad.ac.id.

Mohd Hatta Jopri received his Bachelor of Engineering. from Universiti Teknologi Malaysia (UTM), M.Sc. in Electrical Power Engineering from Rheinisch-Westfälische Technische Hochschule Aachen (RWTH), Germany, and Ph.D. degree from Universiti Teknikal Malaysia Melaka (UTeM), respectively. Since 2005, he is an academia and research staff at UTeM. He is registered with Malaysia Board of Technologist (MBOT), Board of Engineers Malaysia (BEM) and a member of International Association of Engineers (IAENG). His research interests include power electronics and drive, power quality analysis, signal processing, machine learning, and data science. He can be contacted at email: hatta@utem.edu.my.